Diyala Journal of Engineering Sciences

Journal homepage: https://djes.info/index.php/djes

ISSN: 1999-8716 (Print); 2616-6909 (Online)

Development of a Comprehensive Frequency Control Model for the GB Power System: A Research and Educational Tool

Ali Sachit Kaittan*, Zeyad Assi Obaid and Ali Najim Abdullah

Department of Electrical Power and Machines Engineering, University of Diyala, 32001 Diyala, Iraq

ARTICLE INFO

Article history:
Received May 30, 2024
Revised December 4, 2024
Accepted December 24, 2024
Available online March 1, 2025

Keywords:
Frequency control
Generating unit
DERs
Multi-machines power systems
Tie-lines

ABSTRACT

A modelling of three interconnected areas based on Great Britain's (GB) power system for frequency control offered a wide range of stability analyses for both under and postgraduate studies. The system inertia was counted according to the generation amount for the current system and the year 2035. The areas were assigned according to the GB transmission boundaries. This includes the north zone which is above the B7a boundary, the South is below the B9 boundary, and the Midland is in between. Each area has an aggregated model of each generation for Gas, Coal, Hydro, Nuclear, wind, and others as well as an aggregated load. The wind farms were divided into offshore and onshore and did not participate in frequency regulation or ancillary services. Automatic Generation Control (AGC) was used in each area to regulate the area frequency according to the system frequency. Area Control Error (ACE) was used in the proposed model as the total summation of the area frequency error alongside the power deviation of the transmission lines (tie-lines) with other areas. The main goal was to evaluate the effect of power system stabilizers (PSS) on system stability under disturbances, such as three-phase faults and resonance conditions. Results showed that wide-band PSSs offer superior stability by effectually damping low-frequency oscillations, while Delta PSS established better performance in mitigating the impact of generator resonance. The outcomes highlight the importance of integrating modern PSSs in large generators to improve dynamic stability and reduce the risks associated with resonance. The proposed package will be offered for free when requested for students and staff to conduct different analyses.

1. Introduction

The frequency control of power systems has become gradually critical due to the developing nature of energy grids, marked by higher integration of renewable energy sources and reduced system inertia. The researches underscore the complexities and evolving challenges of frequency control in modern power systems, particularly within the GB context. There is a strong need for advanced control strategies and comprehensive simulation models to provision the ongoing transition to a more sustainable and resilient power grid. This paper contributes to this field by developing a comprehensive frequency control model that addresses the exceptional dynamics of the GB power system, providing a valuable tool for research and educational purposes. Reference [1] was the early research papers dealing with frequency control for the GB grid definitely, focused on traditional centralized methods and system inertia. This research addresses the exclusive aspects of frequency control in the GB grid, considering its generation mix and control methodologies. An early investigation to the

* Corresponding author.
E-mail address: alisachit@uodiyala.edu.iq
DOI: 10.24237/djes.2025.18108

This work is licensed under a Creative Commons Attribution 4.0 International License.

dynamic behavior of the GB power system, considering its control strategies and frequency response has been presented in [2].

Traditional power systems relied deeply on synchronous generators, providing inherent inertia that helped stabilize frequency fluctuations. However, studies such as those by Kundur et al. and Machowski et al. highlight that with the growing share of renewable energy sources like wind and solar, the effective inertia of the system has decreased, affectating significant challenges to maintaining frequency stability. These changes require advanced control strategies and system adaptations to ensure reliable grid operation [3,4].

Power System Stabilizers have been widely researched and applied to enhance the dynamic stability of power systems by damping low-frequency oscillations. Studies by Anderson and Fouad show that PSSs advance the performance of generators under transient conditions, contributing expressively to frequency control. Additional research by Aboul-Ela et al. discovered various PSS designs, including Delta PSS and wide-band PSS, showing their effectiveness in different operational scenarios. These stabilizers help respond to the effects of disturbances such as faults and resonances, which are critical for preserving system stability [5-6].

Specific studies concentrating on the GB power system, such as those by National Grid ESO and Milborrow highlight the unique challenges of the region's grid, including a high penetration of offshore wind and the planned reduction of fossil fuel-based generation. These studies detect the need for enhanced frequency response strategies, particularly as the grid develops towards a low-carbon future. Models developed by Ekanayake and Jenkins provide appreciated insights into how different control strategies impact system frequency, emphasizing the importance of simulation tools in predicting system behavior [7-9].

Recent advances in simulation tools, such as those presented by Milano (2005) with Power System Analysis Toolbox (PSAT), permit for detailed modeling of frequency control dynamics. These tools are necessary for testing and validating new frequency response strategies under various grid conditions. They assist in the assessment of PSS designs and their effectiveness in damping oscillations and maintaining grid stability during disturbances [10].

The literature also recognizes emerging trends and technologies in frequency control, including the use of battery energy storage systems (BESS) and innovative grid-forming inverters. Studies like those by Rodriguez-Garcia et al. discuss how these technologies can offer fake inertia and fast frequency response, further stabilizing the power system. This highlights the rising role of advanced solutions in addressing frequency control challenges in modern grids [11-13].

Control of frequency is an important field for both industry and hence, for educational purposes. Recently, a wide range of Distributed Energy Resources (DERs) have been integrated worldwide and added more challenges for this field. These types of resources have difficulties in stability more classic power generators. Some of the DERs provide no inertia due to their power electronics. The analysis of power system stability with these resources is an important aspect of the power systems. The stability of the power system with various DERs can be improved with well-controlled scenarios [14].

The stability of the smart grid power system with different DERs was proposed earlier. An electronics-based DERs with smart loads were considered as well. The classical power system and the stability of power electronics were considered to identify the problems considering steady state, small-signal, and large-signal stability analyses [15-17]. Protection and control devices were used recently in power systems with an intelligent technique alongside DERs as the cutting edge for modernized power systems. Battery energy storage systems are also considered for the stability improvements of frequency control in power systems. are considered in the previous work for the application of frequency regulation in the power system. Various research and review papers presented to analyze the frequency control of power systems such as Great Britain power system. The inertia reduction, the main source of inertia, the challenge in future reduced inertia

systems, as well as the types of possible new control techniques were introduced and discussed [18]. The demand side response alongside the DERs was considered as one of the promising techniques for controlling the frequency in modern power systems. The population of these controllable loads and DERs could be useful in representing such analyses [19].

To ensure the smart grid works well, safely, and reliably, there has been an increase in the use of information and communication technologies (ICT) for live monitoring and management. With these technologies, our system became a complicated cyber-physical system (CPS), where communication networks are important for how well the smart grid (SG) works. So, it's really important to use combined modeling and simulation (IMS) of control and communication systems. This helps us assess the Smart Grid Cyber-Physical System (SG CPS) for new control methods or to choose the right communication technologies for particular uses before we use them on a bigger scale. Reference [20] provides a state-of-the-art literature review about co-simulation, one of the key methods to perform an IMS.

Most renewable energy sources in DC microgrids are not always available, respond slowly to changes, and don't have extra power stored. This leads to uneven power supply and makes it hard to provide quick bursts of energy when needed. To solve these problems, reference [21] suggests a better way to manage power using a method called droop control with DC bus signaling (DBS). This approach helps handle power changes on its own for small power systems (microgrids) that can operate both by themselves (islanded) or connected to a larger grid, without needing a central controller or communication systems. Also, the suggested better droop control divides the load power into temporary power and steady power for the supercapacitor, battery, and grid.

The availability of a free-access educational package is important to broaden the knowledge of both professionals and individuals. However, there is a difficulty for them to harness the benefits of such studies due to the cost of different packages. There are different packages proposed in the literature with missing data and details as explained earlier. These models were presented to test developed tools rather than to study the dynamic stability. Also, there is a wide range of unidentified purposes for these packages or it was presented without free access [22-24].

Therefore, this paper presents an educational package to study and analyze wide stability issues in multi-machine power systems. The presented model was modeled and implemented using MATLAB Simulink to offer a wider range of stability analysis. The model displays the output of all generators and their data where it is recorded dynamically. The design provides a simple way of studying for academic purposes [25]. The main aim of the proposed package can be summarized as follows:

1. It offers a wide range of stability analyses for both transient and steady-state studies in the field of power system stability and control.
2. The model is with full-detailed machines, loads, and transmission lines, hence, presenting a more accurate analysis.
3. The model is based on a very known benchmark power system with full realistic data and hence, offers more simplicity for students and researchers.
4. The model is dynamic and, therefore, offers more flexibility to test and apply different power system technologies, such as Wind, Solar, Biomass, Flywheel, and controllable loads.
5. The model was built to broaden the resources of the studies in the College of Engineering, University of Diyala, also, it is available for free for others when requested.

2. Frequency control model

The analysis of the frequency control is achieved by the basic speed governor mechanism, this mechanism can by shown by considering an isolated generating unit connected to a local load as shown in Figure 1.

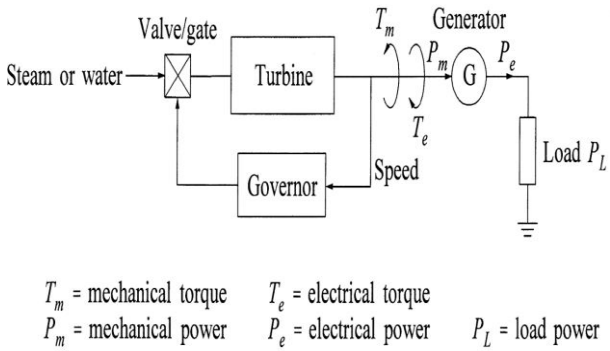

Figure 1. Governor-Turbine model as a generating unit supplying an isolated load [3].

The load change is reflected as a change in the electrical torque output *Te* of the generator. Thus, there will be a mismatch between the mechanical torque *Tm* and the electrical torque *Te* which in turn results in speed variations. The relationship between the rotor speed as a function of the electrical and mechanical torques is shown in Figure 2.

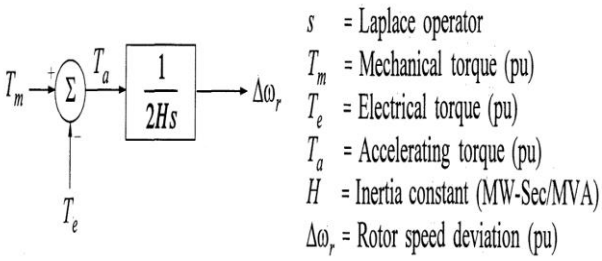

Figure 2. Speed and Torque Relationship [3].

For load-frequency control (LFC) analysis, it is preferable to express this relationship in term of mechanical and electrical power (P) rather than torque (T). The load Damping constant (D) is expressed as a percent change in load for one percent change in frequency. Typical values of D are from 1 to 2 percent. A value of D=2 means that a 1% change in frequency would cause a 2% change in load. The system model with the effect of the load damping is shown in Figure 3[22-25].

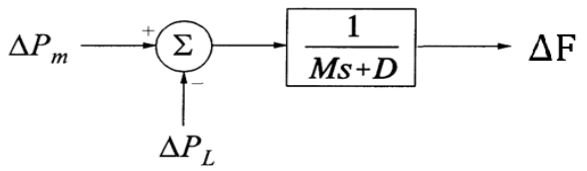

Figure 3. System Model with the Load Damping Constant [3].

Where:

$M=2H$
ΔP_m: The change in mechanical power.
ΔP_L: The load change.
ΔF: The system frequency deviation.

The frequency response can be represented by several low-order models. The system model as shown in Figure 3 is the same in all frequency control analyses, the typical value of D=1 is used in the literature. However, the inertia constant value (M=2H) has an important effect on the system frequency response, and it is counted according to the generation type and capacity. The Turbine-Governor model has different types and can be represented by several low-order model in s-domain. This model represents a turbine-governor model in a synchronous generator. A synchronous governor adjusts the turbine valve/gate to bring the frequency back to the nominal or scheduled value. Figure 4 shows a system response of a generating unit with synchronous governor when subjected to an increased load. As a speed drops, the turbine mechanical power begins to increase. The speed will ultimately return to its reference value and the steady-state turbine power increases by an amount of the additional load.

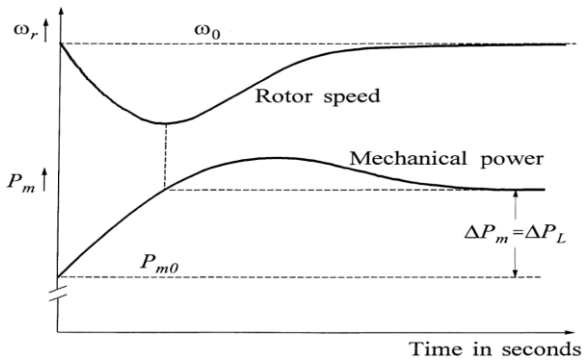

Figure 4. System Response of a generating unit with synchronous governor [3].

In LFC analysis, ΔP_m is a summation of each individual generator in the area. This enables the System Operator (SO) to control each generation unit and to provide an ancillary service (see Figure 5).

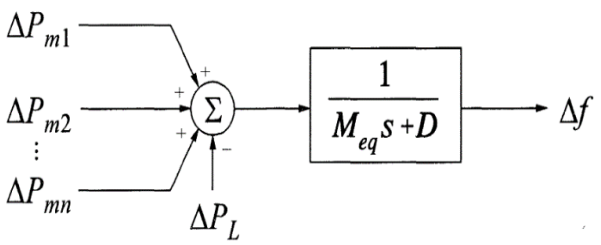

Figure 5. A collective of generators [3].

The equivalent of the system inertia (*Meq*) is equal to the sum of the inertia of each individual generator. Similarly, the effect of the load damping coefficient is represented by a single value of D. In this research, the non-reheat steam turbine model is used to represent the generation units of each individual type with steam turbine (see Figure 6).

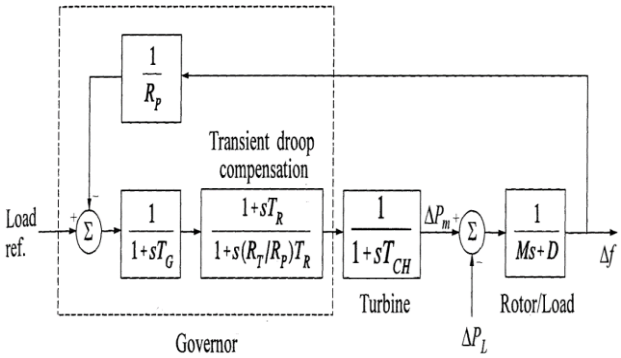

Figure 6. Frequency control with non-reheat steam turbine-governor model [3].

For the best frequency control, a droop compensation block was used between the governor and the turbine models. The hydraulic turbine model was used to represent the hydraulic and the pump-storage generation units (see Figure 7) [22-25].

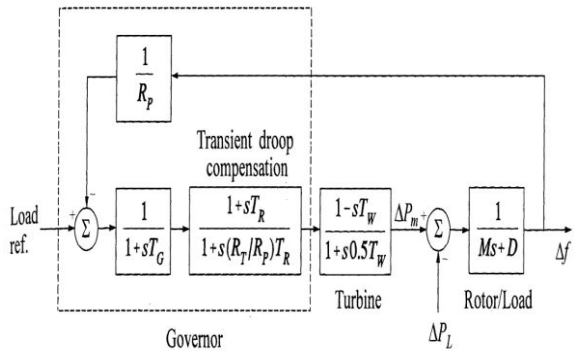

Figure 7. Frequency control with Hydraulic turbine-governor model [3].

Wind Turbine Generators (WTGs) were used as an aggregated model as a single generator collected with ΔP_m, however, WTGs will not participate in regulating the frequency and are counted as a zero inertia [25-28]. The aggregator model of the WTGs was represented by three first order models for the wind generator, the interface (I/C), and the invertor (IN) as shown in Eq.1 [25-28].

$$G(s)_{WTGs} = \left(\frac{K_{WTG}}{1+sT_{WTG}}\right) * \left(\frac{1}{1+sT_{\frac{I}{C}}}\right) * \left(\frac{1}{1+sT_{IN}}\right) \quad (1)$$

3. Modelling of three Areas GB power system

In the GB power system, the system operator National Grid (NG) has set rules for frequency response. Mandatory Frequency Response (MFR) is an automatic change in active power output in response to a frequency change. This service is used to keep the frequency within the limit (49.5Hz - 50.5Hz) and operational limits (49.8Hz - 50.2Hz). All generation units caught with the requirements of the grid code must provide this service in order to be connected to the transmission system. This can be done by the following frequency loops [22-25].

- Primary Response: increasing the active power or decreasing the demand within 10 seconds after any event can be extended for an extra 20 second.
- Secondary response: increasing the active power or decreasing the demand of the active power within 30 second after any event and can be extended for extra 30 minutes.
- High frequency response: decreasing the active power within 10 seconds and can be extended indefinitely.

NG provide another accessible service related to the frequency response called Reserve Services. The service comprises either generation or demand reduction to be able to deal with unforeseen demand increases and/or generation unavailability. The sources are available to the NG as a reserve and consist of synchronized and non-synchronized sources. The demand side response is out of the scope in this research, the synchronous generation units

are used to provide this automatic service as an increase or reduction in the active power.

MFR providers must have a 3-5% governor droop characteristic and be capable of providing continuous modulation power responses to deal with the frequency changes via synchronised generation through their automatic governing systems. All large generation units must have a MFR (National Grid: =>100MW, Scottish Power: =>30MW, and Scottish Hydro Electricity Transmission: =>10MW).

Thus, not all of the generation units will have an AGC, some of them will be connected only with the primary loop [National Grid]. In the real power system, AGC or Load Frequency Control (LFC) is placed in the secondary frequency loop which is named as a supplementary frequency control to correct the error of the primary frequency loop.

The wide area power system can be represented by multi areas connected by high voltage transmission lines (tie-lines) (see Figure 8 and Figure 9) [26-32].

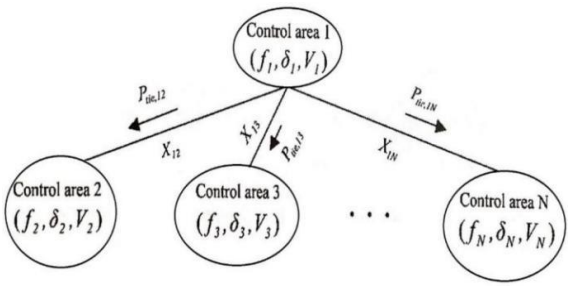

Figure 8. Typical multi-areas power system [3].

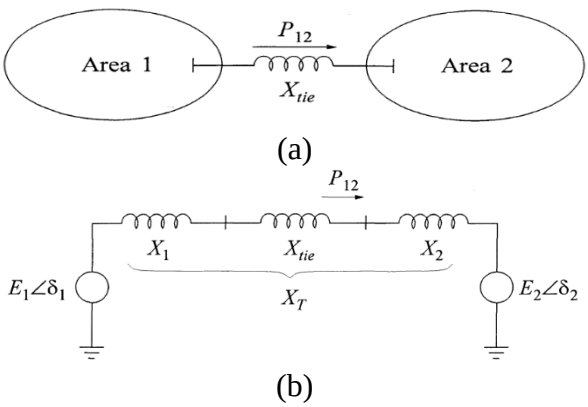

Figure 9. Two area power system, (a) general representation, (b) circuit equivalent [3].

The power interchange between them can be achieved by a wide area monitoring system that provides a scheduled power for each area and for the individual generation units. Each area has a local AGC to regulate the local frequency with respect to the whole system frequency (see Figure 10).

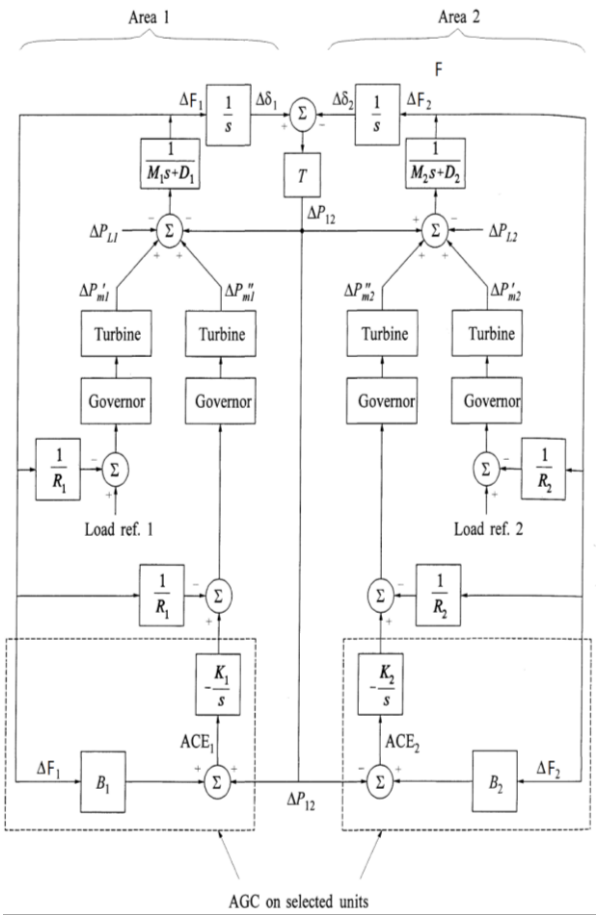

Figure 10. Two areas power system with primary and secondary (AGC) frequency control [3].

Only the large generation units will be connected into the AGC. However, in this research, all units are representing an aggregated generation type as a synchronous unit and will be connected through AGC.

Area Control Error (ACE) is the total summation of the area frequency deviation (ΔF_i) and the power deviation of the tie-line ($\Delta p_{tie,i}$) (see Eq.2). The power deviation of the tie-lines is the summation of the deviation of the local area and other areas (see Eq.3 and Eq.4) [33-35].

$$ACE_i = \beta_i \Delta F_i + \Delta p_{tie,i} \quad (2)$$

$$\Delta p_{tie,i} = \frac{2\pi}{s}\left[\left(\sum_{j=1}^{N} T_{ij} * \Delta F_i\right) - \left(\sum_{j=1}^{N} T_{ij} * \Delta F_j\right)\right] \quad (3)$$

$$T_{i,j} = \frac{|E_i||E_j|}{X_T} Cos(\delta_i^0 - \delta_j^0) \quad (4)$$

Where:

$\Delta p_{tie,j}$: The power deviation in the tie-lines

T_{ij}: The synchronous torque coefficient.

ACE_j: Area Control Error.

β_j: Frequency Bias constant.

X_T: The total reactance of the tie-lines from area i to area j.

E_i, E_j: The Voltage at equivalent machine's terminals.

δ_i, δ_j: The power angles of equivalent machines of area i and area j.

In this paper, the GB power system was divided into three areas according to the transmission system boundaries. The north area (Area 1) is the area above the B7a boundary, the South area (Area 3) is the area below the B9 boundary, and the Midlands area (Area 2) is between them (see Figure 11).

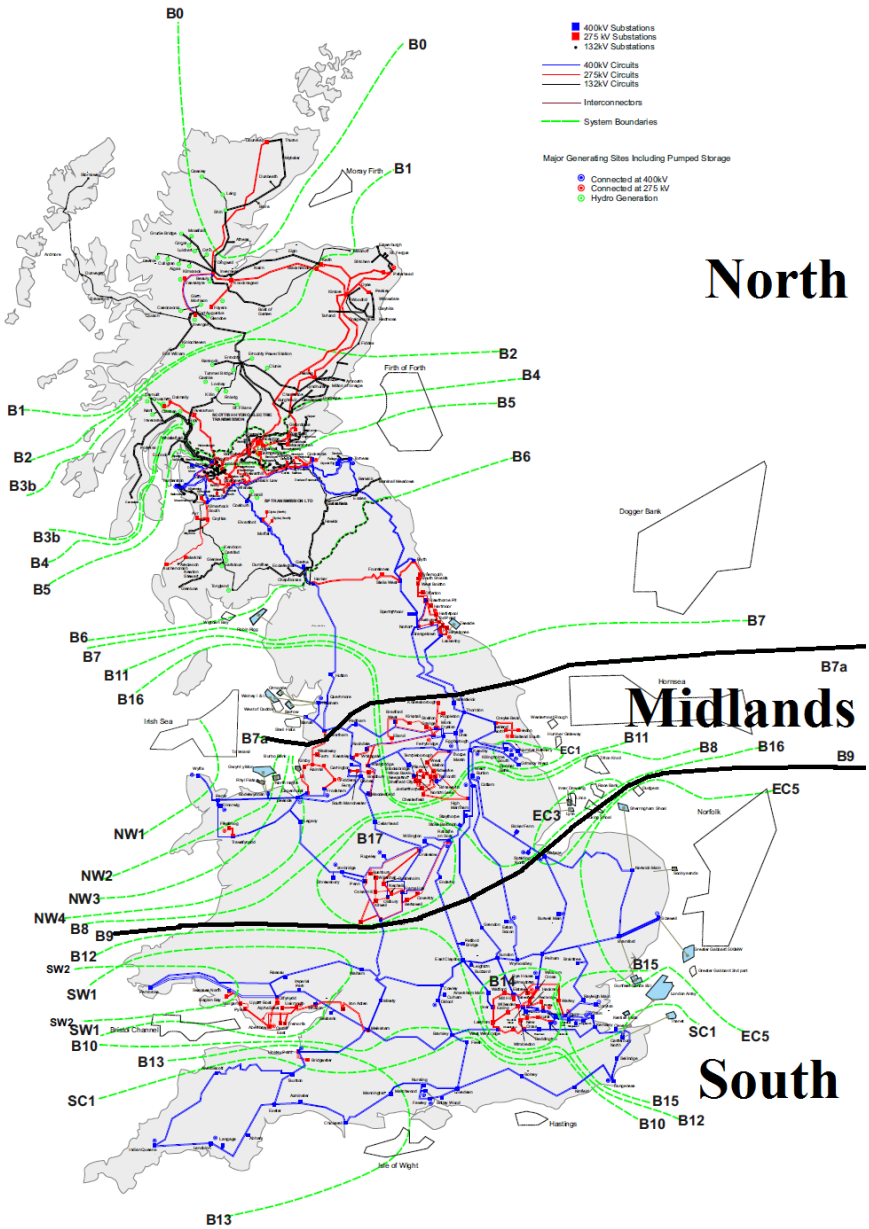

Figure 11. Three Areas GB power system according to the transmission system boundaries [7].

The system inertia of each area was counted according to the total generation of each area. The generation units were aggregated according to the fuel type such as gas, nuclear, coal, hydro, and other. The WTGs were used at each area as an aggregated model to represent the off-shore

and on-shore wind farms [29-32]. The inertia of the WTGs and inter-connectors was counted to zero. The amount of the generated power of each area was calculated according the GB transmission system zones (see Figure 12) and is counted for the year 2035 by using the data of the 2014 electricity ten years statement [33,34].

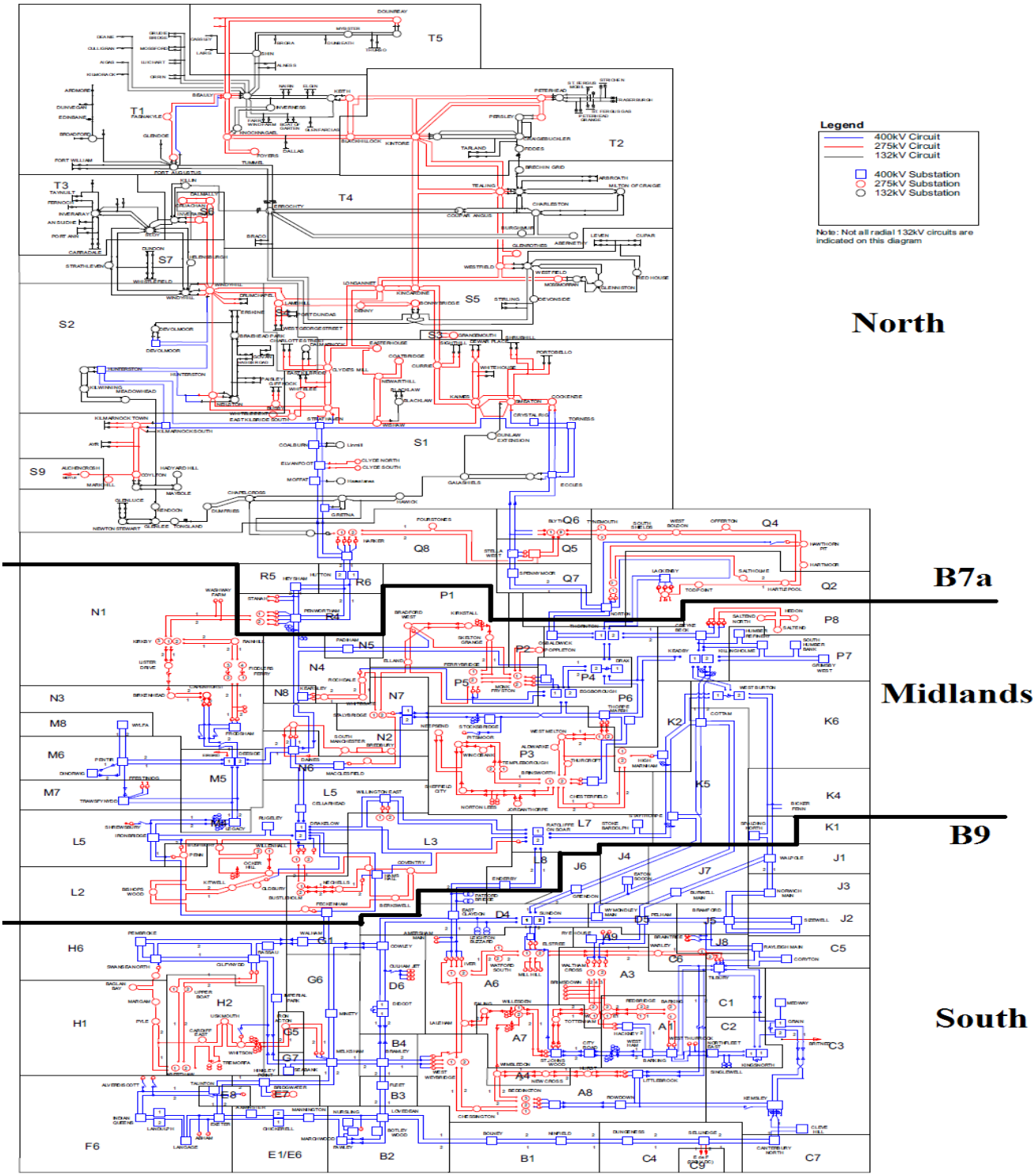

Figure 12. Three Areas GB power system according to the transmission system Zones [7].

Each area has different amount of generation and load. The load demand was represented as an aggregated load of the commercial and domestic load profiles. Each area has many generation units, and each unit represents an aggregated generation type with the per unit ratio according to the total generated power of that area (see Figure 13), where α_i is the participating factor of the unit, and ν_i is the interface with other areas [35-37].

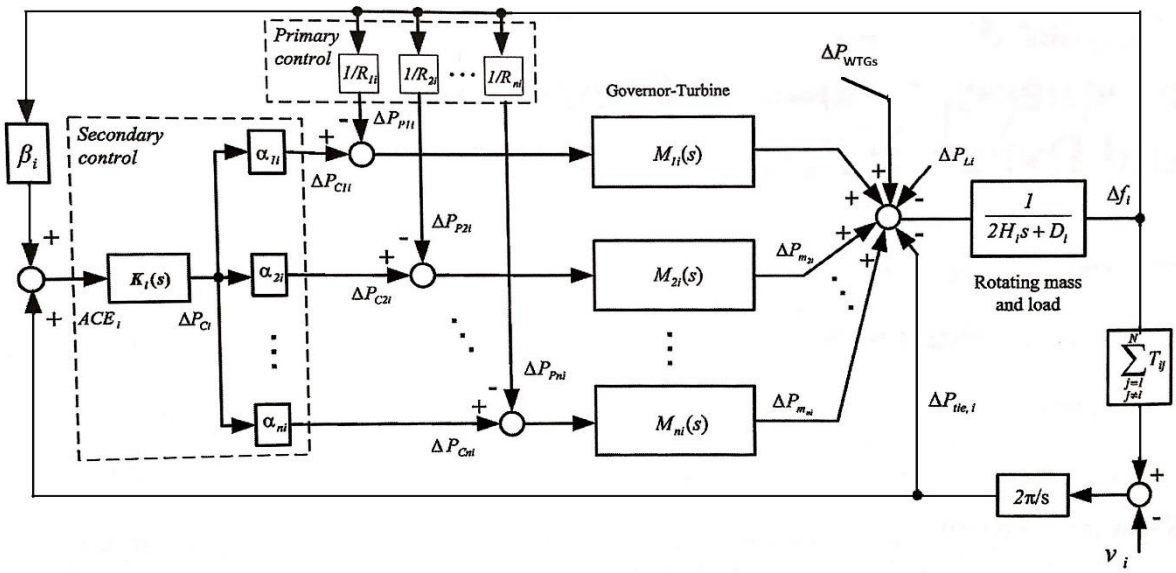

Figure 13. General layout of Area i with different generation units [3].

Each area has a schedule power and load demand for the area and for the tie-lines with other areas (see Figure 14).

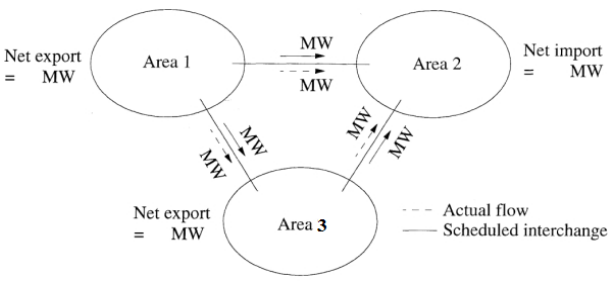

Figure 14. Three areas connected by tie-lines showing the power interchange.

3.1 North Area (Area 1)

This area was represented by aggregating the generation units above the B7a boundary to the north of the GB transmission system. The total amount of the generated power was counted for the year 2035 and it is equal to 20827 MW. This area will have the majority of the wind farms in the GB power system, which is equal to 43% of the total generated power in this area (see Table 1).

Table 1: The aggregated amount of the generation units in the North area [7].

Generation type	Capacity (per unit)
Coal	0.1
Gas	0.04
Hydro pumped and Hydro	0.09
Nuclear	0.27
Offshore Wind	0.1
Onshore Wind	0.33
Other	0.045

The model of this area has five different models represent the aggregated amount of each type as well as the aggregated model to represent the off-shore and on-shore wind farms (see Figure 15), and $G_{c_1}(s)$ is the secondary frequency control (LFC) of area 1.

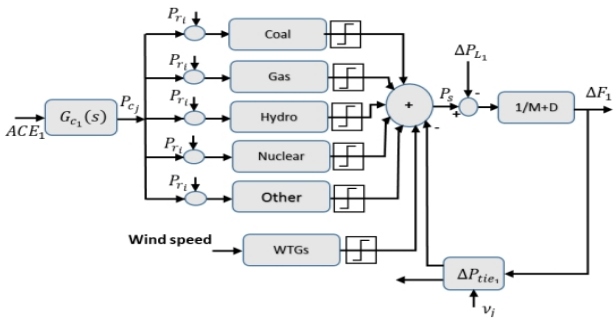

Figure 15. System representation of the North area GB power system.

Where:

$$P_{r_i} = -\frac{1}{R_i} \tag{5}$$

$$P_{c_1} = G_{c_1}(s) * ACE_1 \tag{6}$$

$$ACE_1 = \beta_1 \Delta F_1 + \Delta p_{tie,1} \tag{7}$$

$$\Delta p_{tie,1} = \frac{2\pi}{s}\left(\left(T_{1,2}(\Delta F_1 - \Delta F_2)\right) + \left(T_{1,3}(\Delta F_1 - \Delta F_3)\right)\right) \tag{8}$$

The system inertia was counted according to the area capacity; thus, it has a lower system inertia than other areas due to high WTGs capacity. The equivalent system inertia of this area is equal to 2.067 which means the Inertia constant (M) equal to 4.134 (since M=2H). A comparison was made for the generation capacity of this area in 2015 and the year 2035, the total generation is increased by 32% (see Table 2) due to the increase of the wind and gas generation units [38].

Table 2: Generation capacity of the North Area GB power system [7].

Fuel Type	2014/15 (MW)	2035 (MW)	Variation Range
Coal	2704	2284	-16%
Gas	422	864	105%
Hydro+Pumped	1862	1862	0%
Nuclear	5776	5776	0%
Offshore Wind	788	2170	175%
Onshore Wind	3647.8	6941.1	90%
Other	600	930	55%
Total	15799.8	20827.1	32%

3.2 The Midlands Area (Area 2)

This area was modelled by aggregating the generation units between the B7a and B9 boundaries. The total amount of the generated power for the year 2035 is 30087 MW in this area with the majority of gas and coal fuel (see Table 3).

Table 3: The aggregated amount of each generation units in the Area 2 [7].

Generation type	Capacity (per unit)
Coal	0.32
Gas	0.46
Pumped Storage	0.066
Offshore Wind	0.032
Other	0.11

The model of this area has four different generation units as well as the aggregated model of the off-shore WTGs, and $G_{c_2}(s)$ is the secondary frequency control (LFC) of area 2 (see Figure 16).

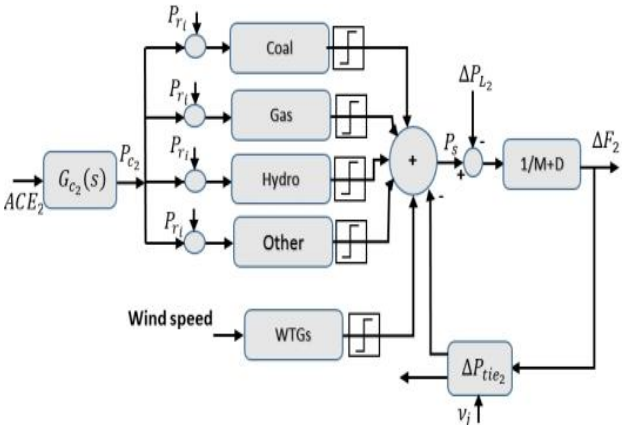

Figure 16. System representation of the Midlands area GB power system.

Where:

$$P_{r_i} = -\frac{1}{R_i} \tag{9}$$

$$P_{c_2} = G_{c_2}(s) * ACE_2 \tag{10}$$

$$ACE_2 = \beta_2 \Delta F_2 + \Delta p_{tie,2} \tag{11}$$

$$\Delta p_{tie,2} = \frac{2\pi}{s}\left(\left(T_{2,1}(\Delta F_2 - \Delta F_1)\right) + \left(T_{2,3}(\Delta F_2 - \Delta F_3)\right)\right) \tag{12}$$

The total system inertia of this area for the year 2035 is equal to 4.39 (see Figure 10). Thus, the value of M is equal to 8.78 and the value of D is 1. The total generated power is decreased by 4% due to cancellation of a nuclear power station and a reduction in the amount of the coal fuel by 32% (see Table 4) [39].

Table 4: Generation capacity of the Midlands Area GB power system [7].

Fuel Type	2014/15 (MW)	2035 (MW)	Variation Range
Coal	14325	9797	-32%
Gas	11482	13907	21%
Hydro+Pumped	2004	2004	0%
Nuclear	490	0	-100%
Offshore Wind	420	990	136%
Other	2707	3389	25%
Total	31428	30087	-4%

3.3 The South area (Area 3)

This was modelled by aggregating the generation units from the B9 boundary to the south of the GB power system. The total generated power is 36021MW with the majority of the gas fuel for about 63% from the total generated power (see Table 5).

Table 5: The aggregated amount of each generation units in the Area 3 [7].

Generation type	Capacity (per unit)
Gas	0.63
Nuclear	0.18
Pumped Storage	0.095
Offshore Wind	0.0063
Other	0.084

The system model of this area has three different generation units as well as the aggregated model of on-shore and off-shore WTGs, and $G_{c_3}(s)$ is the secondary frequency control (LFC) of area 3 (see Figure 17).

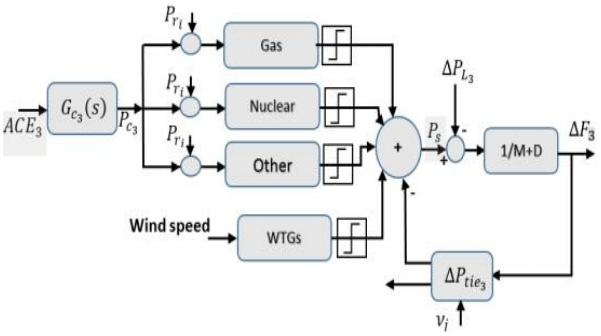

Figure 17. System representation of the South area GB power system.

Where:

$$P_{r_i} = -\frac{1}{R_i} \tag{13}$$

$$P_{c_3} = G_{c_3}(s) * ACE_3 \tag{14}$$

$$ACE_3 = \beta_3 \Delta F_3 + \Delta p_{tie,3} \tag{15}$$

$$\Delta p_{tie,3} = \frac{2\pi}{s}\left(\left(T_{3,1}(\Delta F_3 - \Delta F_1)\right) + \left(T_{3,2}(\Delta F_3 - \Delta F_2)\right)\right) \tag{16}$$

The total system inertia for the 2035 in this area is equal to 4.33 (see Figure 18), and thus the value of M and D are 8.66 and 1, respectively. The total generated power is increased by 25% from the current capacity (see Table 6) [40].

Table 6: Generation capacity of the South Area GB power system [7].

Fuel Type	2014/15 (MW)	2035 (MW)	Variation Range
Coal	1569	0	-100%
Gas	18002	22796	27%
Nuclear	3205	6546	104%
Offshore Wind	2160	3400	57%
Onshore Wind	0	228	100%
Other	3856	3051	-21%
Total	28792	36021	25%

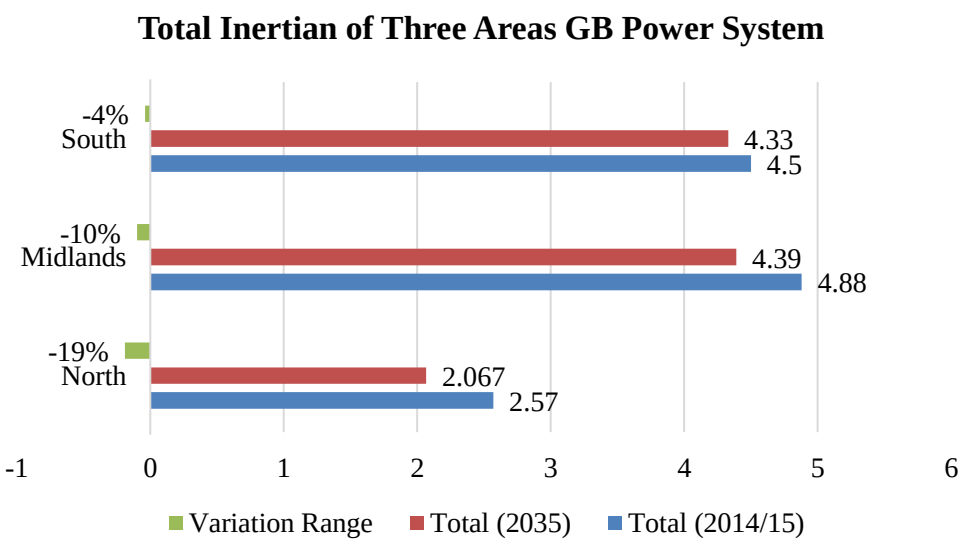

Figure 18. Inertia comparison of three areas GB power.

The total inertia of the three areas has varied from the current amount and in the year 2035, the generation units with gas fuel have the highest value of inertia while the WTGs and the interconnectors were counted to zero inertia. Area 2 has the highest inertia than other due to the low amount of the WTGs. Totally, all of the three areas have a reduction in the inertia value from the current system to the year 2035 (see Figure 18).

The model of the three areas GB power system was designed in MATLAB/Simulink, and the initialization of the parameters was done by the programming M-file. Each area has four inputs (three outer and one inner) and one output. The inputs are: area load demand, area wind mechanical power, and two other inputs represent the frequency deviation of other areas. The one output is the area frequency deviation which goes to other areas as an input (see Figure 19).

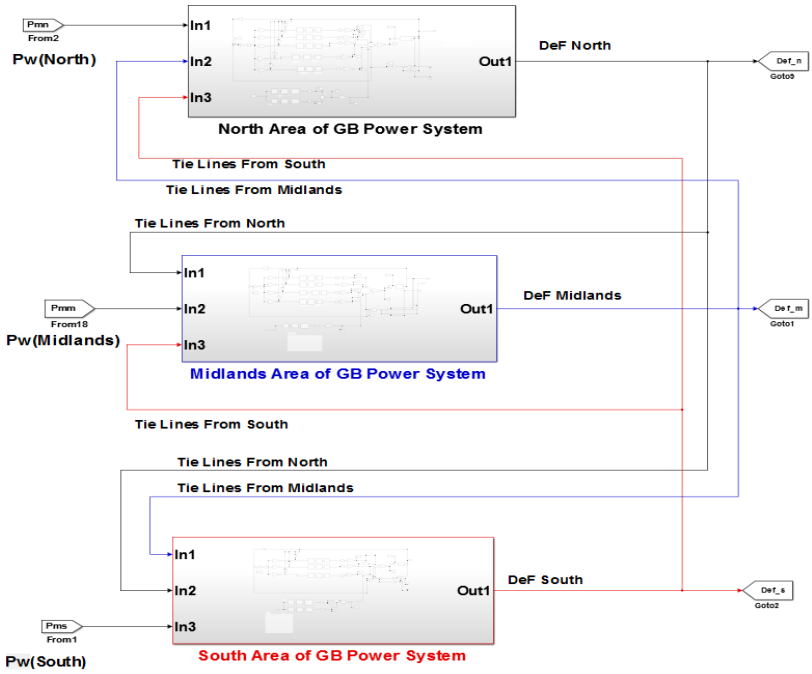

Figure 19. The model of the three areas GB power system.

As equations 7, 11, and 15, if the total tie-lines power deviation of the area ($\Delta p_{tie,j}$) was positive, that means it will be counted as a load to the area.

When $\Delta p_{tie,j}$ acts as a load, which means the area power is bigger than the area load and bigger than the generated power of other areas. The difference will be transferred to other areas by the tie-lines to compensate for the unbalance in other areas and to keep the frequency the same as in all areas. Each area has the general layout of Fig.13 and the generation unit's models are as in Figures 15, 16, and 17. The hydro model was resented by the hydraulic turbine-governor model as shown Fig.7 while other units were represented as non-reheat steam turbine-governor models as shown in Figure 6.

The final model of MATLAB Control and monitoring panel of the three areas GB power system can be seen in Figure 20. The monitoring panel is to display the details about the generation units, its power amount, areas frequency, tie-lines power, and ACE as well as to control the areas' load and wind speed [41-46].

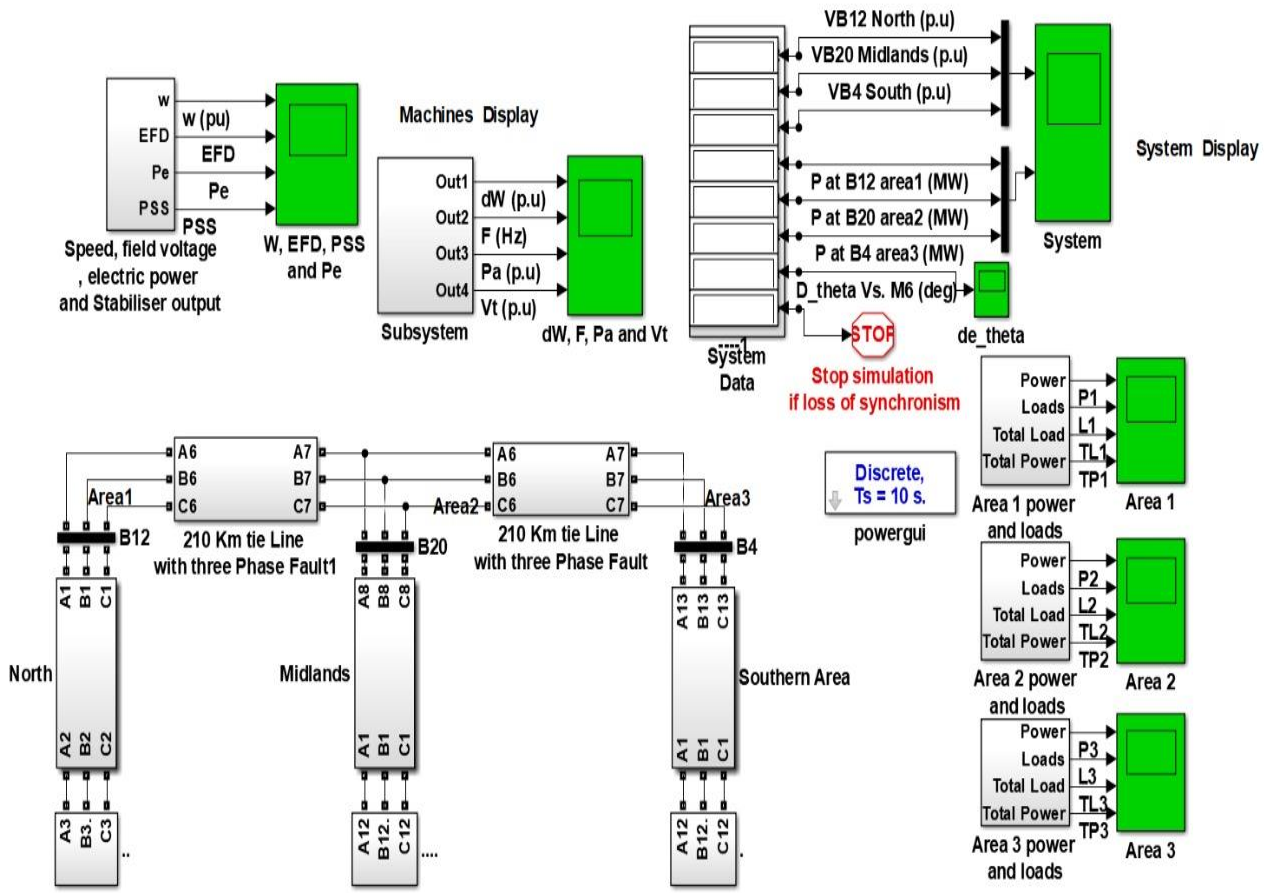

Figure 20. MATLAB Control and monitoring panel of the three areas GB power system.

3. Results and discussion

The study case was used to test the modelled three areas GB power system with real demand of the GB power system. The data of this test was taken from the U.K. National Grid Status website on Saturday 7th of December 2014 since the weekend in December usually have the largest load demand. A per unit load was counted according to the total demand and generation every 5 minutes of 24:00 hours weekday. This load was used as an input load at each area of the GB power system. The monitoring panel was designed to display various system outputs for all generators and loads as well as transmission lines.

The system inertia in this study case was counted according to the current amount and type of generation units. The proposed study cases cover various scenarios for both transient and steady-state response analyses. In this paper, the cases focus on the impact of different power system stabilizers (PSS) which were used in each generator. A disturbance was applied to the system as a sudden generation loss. The following plots show some generators' results with different types of power system stabilizers by applying three phase faults at 2_3 tie lines. The integrated PSSs are used in different power systems to damp the low-frequency oscillation in the generator. Figure 21 proves how different models handle a severe grid disturbance like a three-phase fault. The 2035 models clearly outperform the 2015 models, exhibiting better frequency control and faster stabilization. The wide band PSS (1iMB) presented better stability for generator 1 in the north area than the others due to its design structure which offers a different range of frequency oscillations.

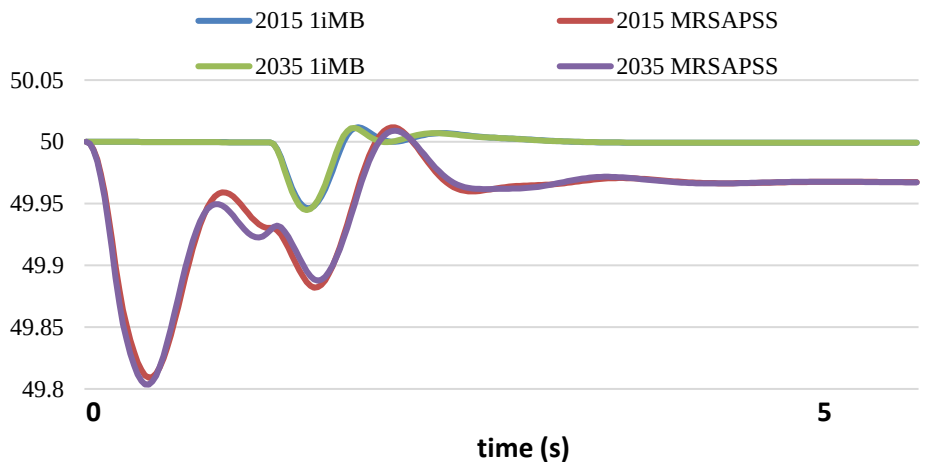

Figure 21. Generator 1 North area (Y-axis is frequency, X-axis is time).

Generator 2 in the north area was assessed for its response to disturbances with diverse power system stabilizers (PSS) applied. The results in Figure 22 suggest that the Model-reference adaptive PSS (MRSAPSS) configuration provides better damping and stability across different years, while the Multiband stabilizer shows more oscillations and slower recovery, particularly in future scenarios (2035). Like generator 1, generator 2's stability was highly influenced by the type of PSS used. The wide-band PSS was verified effective in damping low-frequency oscillations, contributing to a stable operation throughout fault conditions.

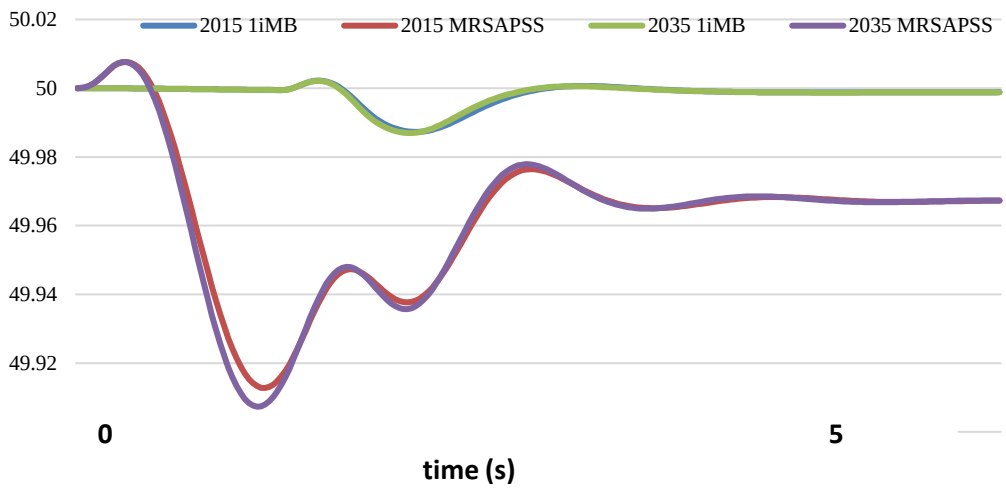

Figure 22. Generator 2 North area (Y-axis is frequency, X-axis is time).

In Figure 23 generator 1 in the south area was evaluated under the same conditions to evaluate its dynamic stability. The Model-reference adaptive PSS consistently outperforms the Multiband stabilizer in both the 2015 and 2035 scenarios, providing better damping and stability by minimizing frequency deviations and ensuring faster recovery. This suggests that the MRSAPSS is stronger in maintaining system stability as the power system evolves. The wide-band PSS was chiefly effective in stabilizing the generator by damping low-frequency oscillations during fault conditions. This contributed to a smoother and more stable operation.

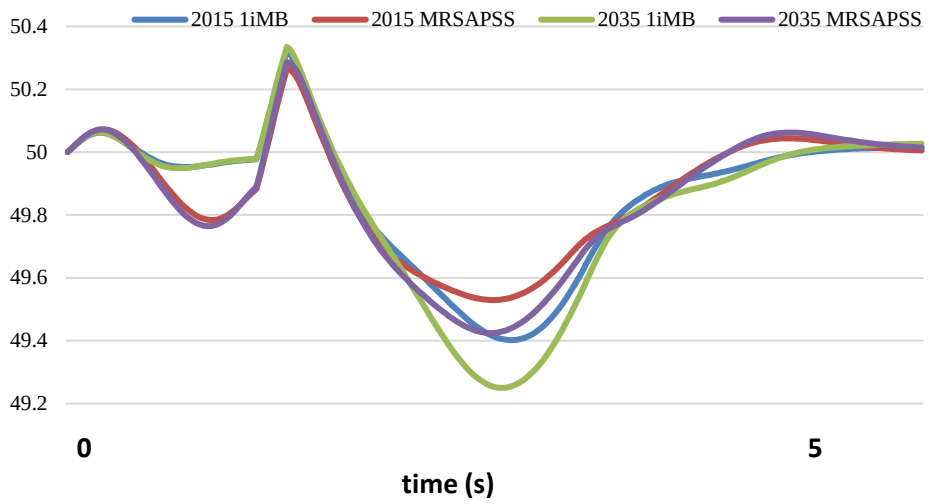

Figure 23. Generator 1 South area (Y-axis is frequency, X-axis is time).

The MRSAPSS in Figure 24 consistently offers better frequency stability for Generator 2 in the south area compared to the 1iMB stabilizer, especially in the projected 2035 situation. It effectively dampens oscillations and advances the system's dynamic response, emphasizing its advantage in maintaining system stability under changing conditions. The analysis revealed that the generator's stability was highly dependent on the type of PSS implemented. The result shows that the wide-band PSS provided operative damping of low-frequency oscillations, leading to a more stable response throughout transient disturbances like three-phase faults.

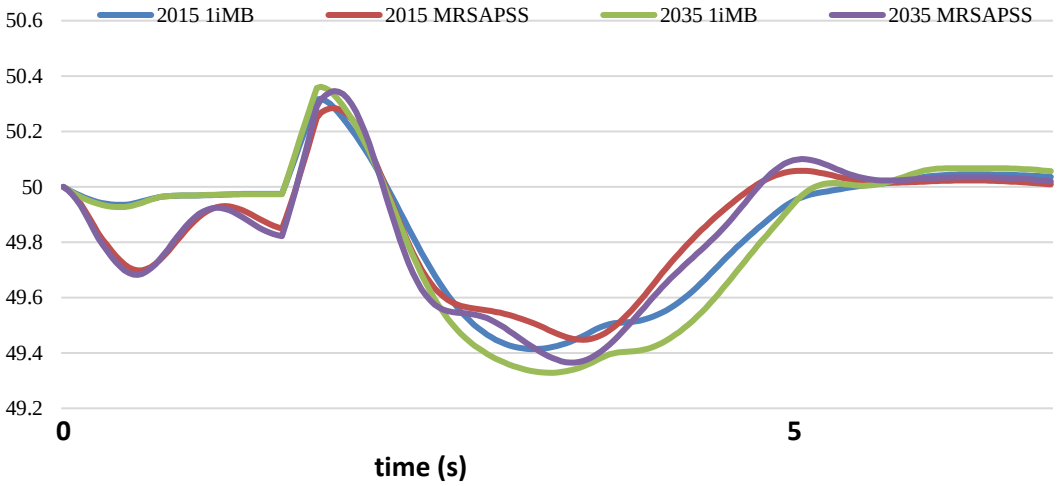

Figure 24. Generator 2 South area (Y-axis is frequency, X-axis is time).

The second test is by applying a resonance at a specific generator to compare the impact of the stabilizer type on the dynamic stability of the generators. The resonance test is an important test in power system due to it sever impact on the generator shaft. The resonance in the generator can be seen as a low-frequency oscillation, therefore, integrating modern PSS in large generators can reduce the impact of the resonance. Figure 25 shows that Delta PSS presented a better response than others in generator 1. Delta W PSS indicates the speed of the generator 1 shaft and, therefore, indicates the resonance that appears on the shaft.

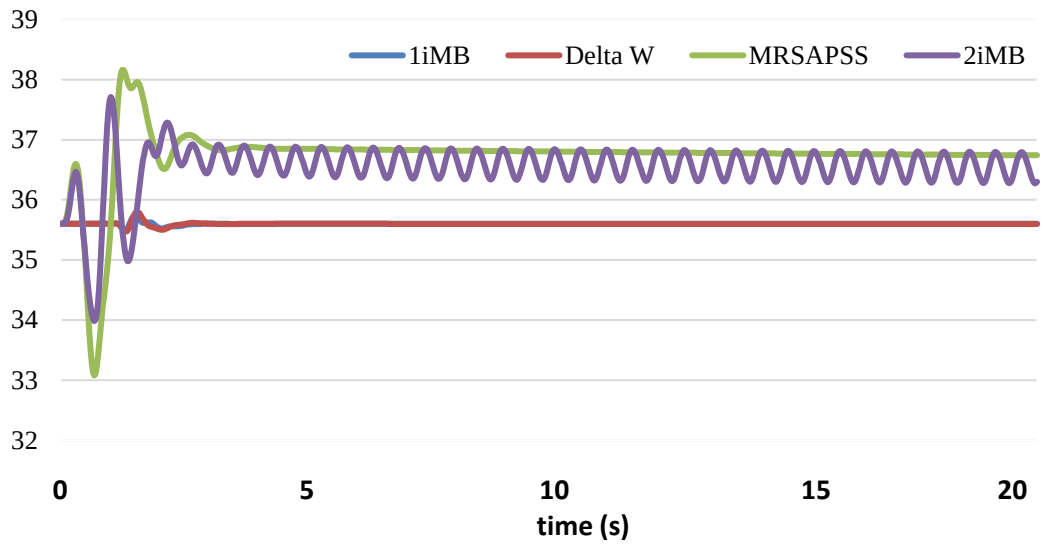

Figure 25. Generator 1 North area (Y-axis is power output, X-axis is time).

However, when resonance was hosted, in Figure 26, Delta PSS showed better performance by dropping the impact of resonance on generator 2's shaft. This highlights the critical role of the Delta PSS in keeping dynamic stability, mainly in scenarios where resonance poses a risk. The findings suggest that choosing the appropriate PSS is essential for ensuring the reliable operation of generator 2 in the power system.

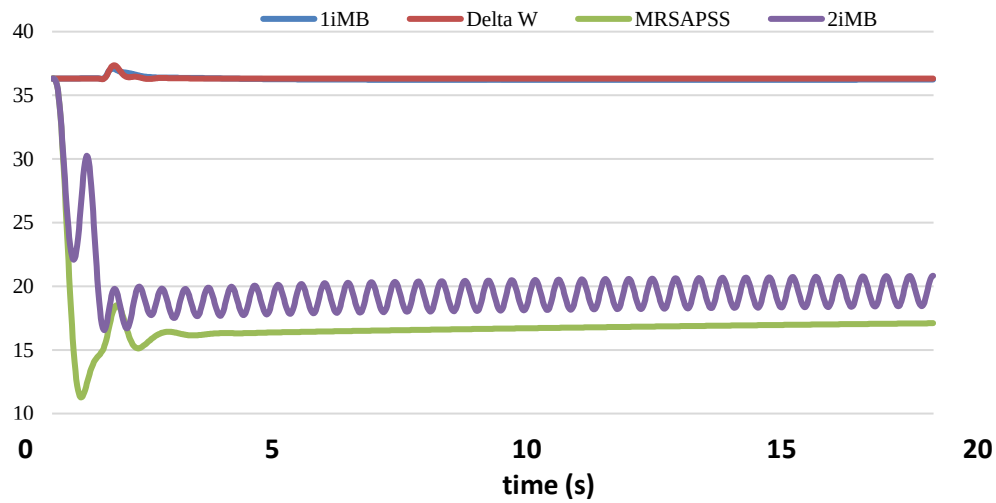

Figure 26. Generator 2 North area (Y-axis is power output, X-axis is time).

When subjected to resonance tests, the Delta PSS showed higher performance by effectively minimizing the impact of resonance on the generator's shaft. These findings underscore the importance of using modern PSS designs, like the wide-band and Delta PSS, to enhance the stability and reliability of Generator 1 in the south area, particularly under challenging operating conditions and Figure 27 approves that.

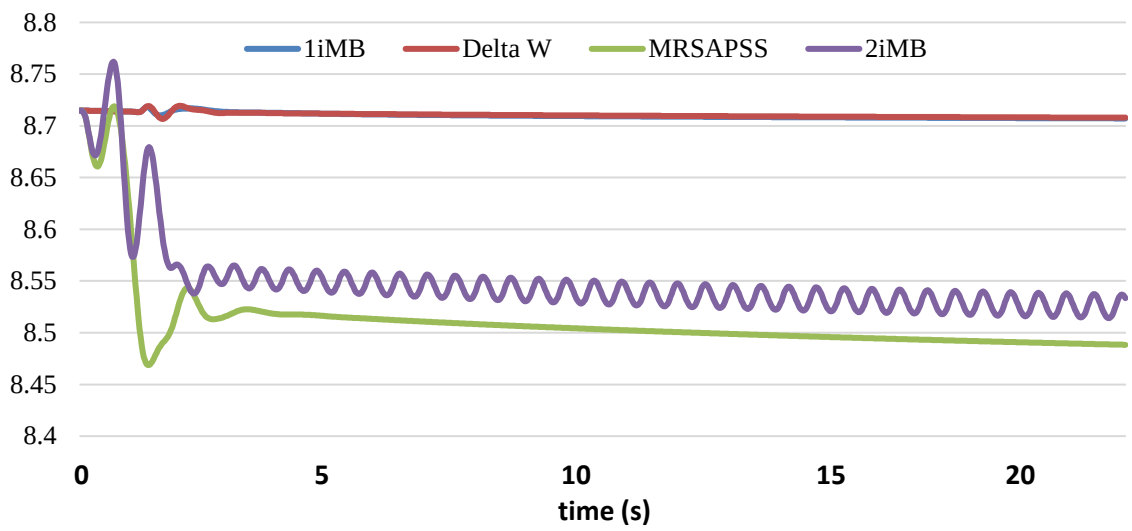

Figure 27. Generator 1 South area (Y-axis is power output, X-axis is time).

During resonance checks, the Delta PSS outperformed other stabilizers by reducing the opposing effects on the generator's shaft, thereby enhancing its dynamic stability. The results in Figure 28 highlight the importance of choosing the appropriate PSS for Generator 2 in the south area to ensure forceful performance and reliability in the power system, particularly in scenarios involving resonance and other dynamic disturbances.

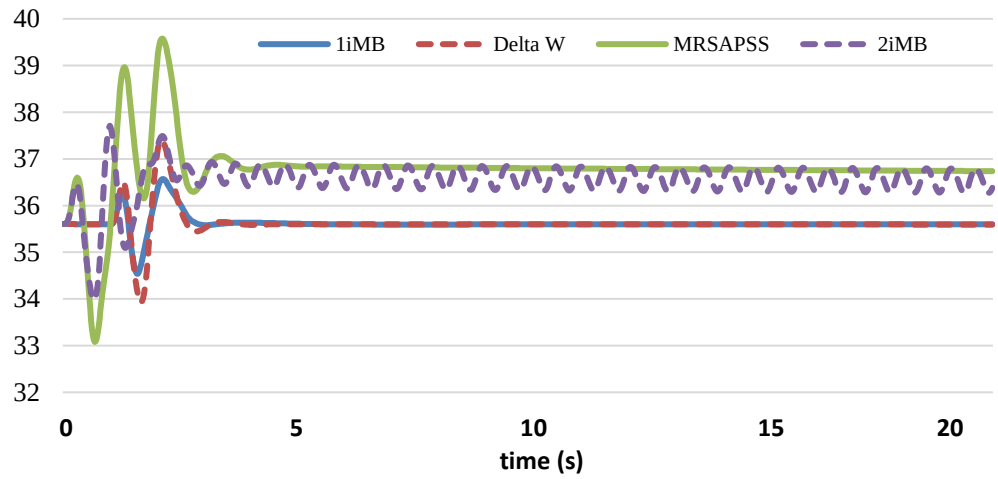

Figure 28. Generator 2 South area (Y-axis is power output, X-axis is time).

4. Conclusions

An educational package was modelled and implemented using MATLAB based on a developed three areas GB power system. The proposed package offers a simple monitoring panel with various study cases for both transient and study state analyses. The proposed educational package offers more flexibility for all under and post graduate studies. The package is available for free by author when requested. The proposed model is presented as a dynamic power system model based on real model and real data. In this paper, the PSS was used to improve the stability analysis following various disturbances. The simulation results showed that integrating a modern PSS could have a great impact on following disturbances. The model is proposed to broaden the knowledge of students and researched for the real events could be happen in future in any power system. In addition, it presents a wide range of stability

analysis. The model could be used later to integrate renewable energy resources and study their locations and impact.

References

[1] M. J. H. Sterling, "Dynamic performance of the UK grid system: Challenges and approaches," Proc. Inst. Elect. Eng., vol. 127, no. 5, pp. 295-301, Sep. 1980.

[2] D. Flynn and M. D. Ilic, "Dynamic response and control of the British power system," IEEE Trans. Power Syst., vol. 6, no. 3, pp. 1165-1172, Aug. 1991.

[3] P. Kundur, N. J. Balu, and M. G. Lauby, Power System Stability and Control. New York, NY, USA: McGraw-Hill, 1994.

[4] J. Machowski, J. W. Bialek, and J. R. Bumby, Power System Dynamics: Stability and Control. Hoboken, NJ, USA: Wiley, 2008.

[5] P. M. Anderson and A. A. Fouad, Power System Control and Stability. Piscataway, NJ, USA: IEEE Press, 2003.

[6] M. E. Aboul-Ela, A. A. Sallam, J. D. McCalley, and A. A. Fouad, "Damping controller design for power system oscillations using global signals," IEEE Trans. Power Syst., vol. 11, no. 2, pp. 767-773, May 1996.

[7] National Grid ESO, Frequency Response Technical Report. London, U.K.: National Grid Electricity System Operator, 2020.

[8] D. Milborrow, "Wind energy and frequency stability: The growing challenge," Renewable Energy Focus, vol. 27, no. 2, pp. 15-19, 2018.

[9] J. B. Ekanayake and N. Jenkins, "Comparison of the response of doubly fed and fixed-speed induction generator wind turbines to changes in network frequency," IEEE Trans. Energy Convers., vol. 19, no. 4, pp. 800-802, Dec. 2004.

[10] F. Milano, "An open-source power system analysis toolbox," IEEE Trans. Power Syst., vol. 20, no. 3, pp. 1199-1206, Aug. 2005.

[11] J. Rodriguez-Garcia et al., "Synthetic inertia control in wind power plants: Stability assessment and grid integration," IEEE Trans. Sustainable Energy, vol. 10, no. 2, pp. 688-696, Apr. 2019.

[12] IEEE Power & Energy Society, Power System Dynamic Performance: Improving Frequency Response Capability. Piscataway, NJ, USA: IEEE Standards, 2021.

[13] M. C. Roberts, et al., "The role of battery storage in frequency response services," Energy Reports, vol. 6, pp. 1258-1265, 2020.

[14] A. Ghafouri, J. Milimonfared, and G. B. Gharehpetian, "Coordinated control of distributed energy resources and conventional power plants for frequency control of power systems," IEEE Trans. Smart Grid, vol. 6, no. 1, pp. 104–114, Jan. 2015.

[15] Y. Rui and Z. Yingchen, "Coordinated optimization of distributed energy resources and smart loads in distribution," in Proc. IEEE Power Energy Soc. Gen. Meeting, Boston, MA, USA, Jul. 17–21, 2016, pp. 1-5.

[16] D. Wu, T. Yang, A. A. Stoorvogel, et al., "Distributed optimal coordination for distributed energy resources in power systems," IEEE Trans. Autom. Sci. Eng., vol. 14, no. 2, pp. 414–424, Apr. 2017.

[17] A. C. Chapman and G. Verbic, "Dynamic distributed energy resource allocation for load-side emergency reserve provision," in Proc. IEEE Innov. Smart Grid Technol.—Asia, Melbourne, Australia, Nov. 28–Dec. 1, 2016, pp. 1-6.

[18] M. Georgiev, R. Stanev, and A. Krusteva, "Flexible load control in electric power systems with distributed energy resources and electric vehicle charging," in Proc. IEEE Int. Power Electron. Motion Control Conf., Varna, Bulgaria, Sept. 25–28, 2016, pp. 1-7.

[19] S. Huang, Q. Wu, Z. Liu, et al., "Review of congestion management methods for distribution networks with high penetration of distributed energy resources," in Proc. IEEE PES Innov. Smart Grid Technol., Istanbul, Turkey, Oct. 12–15, 2014, pp. 1-6.

[20] M.M. Aslam, et al., "Riaz A review of integrated modelling and simulation of control and communication systems in Smart Grid," Computers and Electrical Engineering, vol. 119, Part A, p. 109553, Oct. 2024.

[21] K. Pokharel, et al., "Autonomous transient power management strategy based on improved droop control for DC microgrid, "Electrical Engineering, vol. 104, no. 6, pp. 4321-4334, Dec. 2022.

[22] J. Yang and Y. Wang, "A review of the effects of distributed energy resources and power-electronic controlled loading on distribution network stability," in Proc. IEEE Conf. Ind. Electron. Appl., Hangzhou, China, Jun. 9–11, 2014, pp. 1-6.

[23] A. S. Mohamed, et al., "Adaptive control strategies for frequency stability in low-inertia power systems," IET Renewable Power Generation, vol. 14, no. 5, pp. 597-605, 2020.

[24] J. Zhou, et al., "Impact of renewable energy on GB power system frequency stability," IEEE Trans. Power Syst., vol. 35, no. 3, pp. 2303-2312, 2021.

[25] H. Lee, et al., "MATLAB Simulink modelling for enhanced frequency response in GB power system," IEEE Access, vol. 8, pp. 87945-87955, 2019.

[26] H. Bevrani, A. Ghosh, and G. Ledwich, "Renewable energy sources and frequency regulation: survey and new perspectives," IET Renew. Power Gener., vol. 4, no. 5, pp. 438-457, Sept. 2010.

[27] M. Q. Nawaz, Wei Jiang, and Aimal Khan, “Enhancing Wind Turbine Stability and Performance: A Case Study on Speed Control and

Maximum Power Point Tracking", DJES, vol. 17, no. 1, pp. 1–18, Mar. 2024.

[28] Y. G. Rashid, Ismail, M., Hussein, B., Ibrahim, S., "A Multi-Objective Harmony Search Algorithm for Optimal Allocation and Sizing of Multi-Renewable Energy-Based DG and DSTATCOM in Radial Distribution Systems," (2024) International Review of Electrical Engineering (IREE), vol.19, no. 4, pp. 283-299, 2024

[29] H. Bevrani and S. Shokoohi, "An intelligent droop control for simultaneous voltage and frequency regulation in islanded microgrids," IEEE Trans. Smart Grid, vol. 4, no. 3, pp. 1505-1513, Sept. 2013.

[30] A. P. Apostolov, "Modeling of legacy intelligent electronic devices for UCA based substation integration systems," in Proc. Large Eng. Syst. Conf. Power Eng., Halifax, Canada, Jul. 11–13, 2001, pp. 1-6.

[31] H. D. Nguyen, L. Le, and D. M. Vo, "Frequency control ancillary services in power systems with high penetration of renewable energy," Renewable Energy, vol. 94, pp. 295-305, Aug. 2016.

[32] M. Cheng, S. S. Sami, and J. Wu, "Benefits of using virtual energy storage system for power system frequency response," Appl. Energy, vol. 194, pp. 376–385, May 2016.

[33] Z. A. Obaid, L. M. Cipcigan, and M. T. Muhssin, "Design of a hybrid fuzzy/Markov chain-based hierarchical demand-side frequency control," in Proc. IEEE PES Gen. Meeting, Chicago, IL, USA, Jul. 16–20, 2017, pp. 1-5.

[34] M. T. Muhssin, L. M. Cipcigan, N. Jenkins, et al., "Modelling of a population of heat pumps as a source of load in the Great Britain power system," in Proc. Int. Conf. Smart Syst. Technol., Osijek, Croatia, Oct. 12–14, 2016, pp. 1-5.

[35] S. J. Lee, J. H. Kim, C. H. Kim, et al., "Coordinated control algorithm for distributed battery energy storage systems for mitigating voltage and frequency deviations," IEEE Trans. Smart Grid, vol. 7, no. 3, pp. 1713–1723, May 2016.

[36] S. S. Sami, C. Meng, and W. Jianzhong, "Modelling and control of multi-type grid-scale energy storage for power system frequency response," in Proc. IEEE Int. Power Electron. Motion Control Conf., Hefei, China, May 22–26, 2016, pp. 1-5.

[37] H. J. Mohammed, A. S. Kaittan, L. R. Gainullina, A. I. Jaber, "Effective Temperature on the Electric Breakdown of Transformer Oil," 2024 Conference of Young Researchers in Electrical and Electronic Engineering (ElCon), DOI: 10.1109/ElCon61730.2024.10468080.

[38] A. I. Jaber, A. S. Kaittan, M. W. Abdulwahhab, & D. V. Samokhvalov. "Efficiency Improvement of PM Synchronous Wind Generator Using Field Oriented Control with Model-base Current Observer." International Review of Electrical Engineering (IREE), 19(1), 2024.

[39] M. I. M. Aziz, A. Mohamed, M. A. Hannan, and M. F. Karim, "Frequency Control in Renewable-Dominated Power Systems: A Review and Future Research Directions," IEEE Access, vol. 11, pp. 33104-33122, 2023.

[40] Z. Wang, X. Xiao, X. Wang, J. Guo, and J. Wen, "Coordinated Frequency Control of Power System Based on Virtual Synchronous Generator and Demand Response," IEEE Trans. Power Syst., vol. 37, no. 2, pp. 1421-1432, Mar. 2022.

[41] Z. Zhu, J. Xu, and C. Liu, "Adaptive Frequency Control Strategy for Islanded Microgrids Considering State-of-Charge of Batteries," Int. J. Electr. Power Energy Syst., vol. 128, p. 106707, June 2021.

[42] C. Sun, J. Zhang, Y. Sun, and S. Wang, "Dynamic Frequency Control Method of Isolated Power System Based on Hybrid Energy Storage System," IEEE Trans. Sustain. Energy, vol. 11, no. 4, pp. 2798-2807, Oct. 2020.

[43] A. Alimardani, T. Kerdphol, and M. Watanabe, "A Novel Load Frequency Control Strategy for Future Power Systems with High Renewable Energy Penetration," Renewable Energy, vol. 138, pp. 1072-1080, Aug. 2019.

[44] S. M. Hassan, E. E. Mohamed, and A. F. Zobaa, "Robust Frequency Control of an Islanded Microgrid with High Penetration of Renewable Energy," IEEE Trans. Power Syst., vol. 33, no. 5, pp. 5102-5111, Sept. 2018.

[45] A. Gholami and F. Aminifar, "Hierarchical Frequency Control in Power Systems with a High Share of Renewable Energy Sources," IEEE Trans. Power Syst., vol. 33, no. 6, pp. 6344-6353, Nov. 2018.

[46] A. S. Jafar, G. Abdullah Salman, and A. I. Ismael, "Dynamic Simulation of Three Phase Induction Machines Based on Reduced Order Model for Power Systems Analysis", DJES, vol. 16, no. 2, pp. 134–141, Jun. 2023.